

# Regular Perturbation and Achievable Rates of Space-Division Multiplexed Optical Channels

Francisco Javier García-Gómez and Gerhard Kramer

**Abstract**—Regular perturbation is applied to space-division multiplexing (SDM) on optical fibers and motivates a correlated rotation-and-additive noise (CRAN) model. For  $S$  spatial modes, or  $2S$  complex-alphabet channels, the model has  $4S(S+1)$  hidden independent real Gauss-Markov processes, of which  $2S$  model phase noise,  $2S(2S-1)$  model spatial mode rotation, and  $4S$  model additive noise. Achievable information rates of multi-carrier communication are computed by using particle filters. For  $S=2$  spatial modes with strong coupling and a 1000 km link, joint processing of the spatial modes gains 0.5 bits/s/Hz/channel in rate and 1.4 dB in power with respect to separate processing of  $2S$  complex-alphabet channels without considering CRAN.

**Index Terms**—Capacity, multi-mode, optical fiber, space-division multiplexing.

## I. INTRODUCTION

Space-division multiplexing (SDM) via multi-core and multi-mode transmission considerably increases the capacity of optical fibers [1]. Several experiments reaching 10 Pbit/s have been reported, e.g., see [2]–[4]. The analysis in [5], [6] generalizes to SDM and gives a spectral efficiency upper bound of  $\log_2(1 + \text{SNR})$  bits/s/Hz/channel, where SNR is the signal-to-noise ratio without the fiber nonlinearity and “channel” refers to a complex-alphabet channel.

Various mismatched models have been developed to compute achievable rates for single and dual polarization (1-pol, 2-pol) transmission [7]–[9]. We focus on models based on regular perturbation (RP) [10]–[13] and logarithmic perturbation (LP) [14], [15]. A combined RP and LP model is motivated in [16], see also [17], [18].

We follow [19], [20] and develop an analysis for SDM by using the coupling equations in [21], [22], RP, and an approximation related to LP. The result is a correlated rotation-and-additive noise (CRAN) model with correlated phase noise, spatial mode rotations, and additive noise. We use the model to compute achievable rates for SDM channels.

*Notation:* We use similar notation as in [19] and refer to that paper for details. For instance, we write the Fourier transform of a function  $u(t)$  as  $\mathcal{F}(u(t))$  and the inverse Fourier transform of  $U(\Omega)$  as  $\mathcal{F}^{-1}(U(\Omega)) = \mathcal{F}^{-1}(U(\Omega))(t)$ . For vectors, operators such as  $\mathcal{F}$  and  $\mathcal{F}^{-1}$  are applied entrywise.

## II. SPACE-DIVISION MULTIPLEXING

Each spatial mode has two complex-alphabet channels with the same spatial field distribution but orthogonal polarization.

Date of current version September 28, 2021. This work was supported by the German Research Foundation (DFG) under Grants KR 3517/8-1 and 3517/8-2. (Corresponding author: Francisco Javier García-Gómez.)

The authors are with the Institute for Communications Engineering (LNT), Technical University of Munich, 80333 Munich, Germany (e-mail: javier.garcia@tum.de; gerhard.kramer@tum.de).

Consider  $S$  spatial modes, i.e.,  $2S$  complex-alphabet channels in total.<sup>1</sup> The propagating signal is

$$\mathbf{u}(z, t) = (\mathbf{u}^{[1]}(z, t)^T \quad \mathbf{u}^{[2]}(z, t)^T \quad \dots \quad \mathbf{u}^{[S]}(z, t)^T)^T \quad (1)$$

where  $\mathbf{u}^{[s]}(z, t) = (u^{[s]}(z, t), \bar{u}^{[s]}(z, t))^T$  is the vector of signals of the  $s$ -th spatial mode,  $s = 1, \dots, S$ . The variable  $z$  represents distance and  $t$  is time. We consider the following two propagation scenarios. The models assume that fiber birefringence changes randomly with  $z$  [21].

*Weak Coupling:* the linear coupling among spatial modes is neglected, which is reasonable for multi-core transmission. The propagation equation for spatial mode  $s$  is [21, Eq. (26)]

$$\begin{aligned} \frac{\partial \mathbf{u}^{[s]}}{\partial z} &= j\beta_0^{[s]} \mathbf{u}^{[s]} - \beta_1^{[s]} \frac{\partial \mathbf{u}^{[s]}}{\partial t} - j\frac{\beta_2^{[s]}}{2} \frac{\partial^2 \mathbf{u}^{[s]}}{\partial t^2} + \frac{\mathbf{n}^{[s]}}{\sqrt{g_s(z)}} \\ &+ j\gamma \left( f_{s,s} g_s(z) \|\mathbf{u}^{[s]}\|^2 + \sum_{r \neq s} f_{s,r} g_r(z) \|\mathbf{u}^{[r]}\|^2 \right) \mathbf{u}^{[s]} \quad (2) \end{aligned}$$

where  $\beta_0^{[s]}$ ,  $\beta_1^{[s]}$ , and  $\beta_2^{[s]}$  are the coefficients of the Taylor expansion of the propagation constant  $\beta(\Omega)$  in the angular frequency  $\Omega$ , averaged over the two polarizations. The noise signals  $\mathbf{n}^{[s]} = (n^{[s]}(z, t), \bar{n}^{[s]}(z, t))^T$  are independent Wiener processes in  $z$  such that, in the absence of nonlinearity ( $\gamma = 0$ ), the accumulated noise in a bandwidth of  $\mathcal{B}_{\text{ASE}}$  at  $z = \mathcal{L}$  has autocorrelation function (ACF)  $N_{\text{ASE}} \mathcal{B}_{\text{ASE}} \text{sinc}(\mathcal{B}_{\text{ASE}}(t - t'))$ . The nonlinear coupling coefficients  $\gamma$  and  $f_{s,s'}$  are described in [21]. Note that we have absorbed the factors (8/9) and (4/3) from [21, Eq. (26)] into  $f_{s,s'}$ . The functions  $g_s(z)$  account for attenuation and amplification. Ideal distributed amplification (IDA) has  $g_s(z) = 1$ .

*Strong Coupling:* the linear coupling between modes is strong, i.e., the vector  $\mathbf{u}$  is subject to random unitary transformations that change rapidly with  $z$ . This has an averaging effect that simplifies (2) to [21, Eq. (38)]

$$\frac{\partial \mathbf{u}}{\partial z} = -j\frac{\beta_2}{2} \frac{\partial^2 \mathbf{u}}{\partial t^2} + j\gamma \kappa g(z) \|\mathbf{u}\|^2 \mathbf{u} + \frac{\mathbf{n}}{\sqrt{g(z)}} \quad (3)$$

where  $\mathbf{n}(z, t)$  has the same statistics as  $(\mathbf{n}^{[1,T]}, \dots, \mathbf{n}^{[S,T]})^T$ , the average dispersion coefficient is  $\beta_2 = (\sum_s \beta_2^{[s]})/S$ , and  $\kappa$  is defined in [21].

We develop a SDM-CRAN model for weak coupling. The model for strong coupling is a special case with the parameters  $\beta_0^{[s]} = \beta_1^{[s]} = 0$ ,  $\beta_2^{[s]} = \beta_2$  and  $f_{s,s'} = \kappa$ .

<sup>1</sup>This paper refers to mode-division multiplexing but equation (2) also applies to multi-core transmission under certain conditions [21].

### III. REGULAR PERTURBATION

We expand  $\mathbf{u}^{[s]}$  in (2) in powers of a small perturbation  $\gamma$ :

$$\mathbf{u}^{[s]}(z, t) = \mathbf{u}_0^{[s]}(z, t) + \gamma \Delta \mathbf{u}^{[s]}(z, t) + \mathcal{O}(\gamma^2). \quad (4)$$

The steps are the same as in [19], [20] and we arrive at

$$\mathbf{u}_0^{[s]}(z, t) = \mathbf{u}_{\text{LIN}}^{[s]}(z, t) + \mathbf{u}_{\text{ASE}}^{[s]}(z, t) \quad (5)$$

where  $\mathbf{u}_{\text{LIN}}^{[s]}(z, t) = \mathcal{D}_z^{[s]} \mathbf{u}^{[s]}(0, t)$  and

$$\begin{aligned} \Delta \mathbf{u}^{[s]}(z, t) &= j \mathcal{D}_z^{[s]} \left[ \int_0^z \mathcal{D}_{-z'}^{[s]} \left( f_{s,s} g_s(z') \left\| \mathbf{u}_0^{[s]}(z', t) \right\|^2 \mathbf{u}_0^{[s]}(z', t) \right. \right. \\ &\quad \left. \left. + \sum_{r \neq s} f_{s,r} g_r(z') \left\| \mathbf{u}_0^{[r]}(z', t) \right\|^2 \mathbf{u}_0^{[s]}(z', t) \right) dz \right] \end{aligned} \quad (6)$$

where

$$\mathcal{D}_z^{[s]} u(t) = \mathcal{F}^{-1} \left( e^{j \left( \beta_0^{[s]} - \beta_1^{[s]} \Omega + \frac{\beta_2^{[s]}}{2} \Omega^2 \right) z} \mathcal{F}(u(t)) \right). \quad (7)$$

The effect of  $\beta_0^{[s]}$  is a  $z$ -dependent phase shift, and the effect of  $\beta_1^{[s]}$  is a  $z$ -dependent delay. Similar to [20], the  $2S$  entries of the  $S$  noise signals  $\mathbf{u}_{\text{ASE}}^{[s]}(z, t)$  are independent circularly-symmetric complex Gaussian (CSCG) processes. At the end of the fiber ( $z = \mathcal{L}$ ), their ACF for  $\gamma = 0$  is  $N_{\text{ASE}} \mathcal{B}_{\text{ASE}} \text{sinc}(\mathcal{B}_{\text{ASE}}(t - t'))$ .

We use pulse amplitude modulation (PAM) and wavelength division multiplexing (WDM). The indexes  $c$  of the WDM channels are in the set  $\{c_{\min}, \dots, 0, \dots, c_{\max}\}$ . The center angular frequency of channel  $c$  is  $\Omega_c$ , and the WDM channel of interest (COI) has  $c = 0$  and  $\Omega_0 = 0$ . The transmitted signal of spatial mode  $s$  is

$$\begin{aligned} \mathbf{u}^{[s]}(0, t) &= \sum_{m=-\infty}^{\infty} \begin{pmatrix} x_m^{[s]} s(t - mT - \tau_0^{[s]}) \\ \bar{x}_m^{[s]} s(t - mT - \bar{\tau}_0^{[s]}) \end{pmatrix} \\ &\quad + \sum_{c \neq 0} e^{j\Omega_c t} \sum_{k=-\infty}^{\infty} \begin{pmatrix} b_{c,k}^{[s]} s(t - kT - \tau_c^{[s]}) \\ \bar{b}_{c,k}^{[s]} \bar{s}(t - kT - \bar{\tau}_c^{[s]}) \end{pmatrix} \end{aligned} \quad (8)$$

where  $T$  is the symbol period. The base pulse  $s(t)$  has most of its energy in the frequency band  $|\Omega| \leq \pi \mathcal{B}$ . The channels may have different delays  $\tau_c^{[s]}$  and  $\bar{\tau}_c^{[s]}$ . The transmit symbols of the COI ( $c = 0$ ) are  $x_m^{[s]}$  and  $\bar{x}_m^{[s]}$ , and the transmit symbols of the interfering frequencies are  $b_{c,k}^{[s]}$  and  $\bar{b}_{c,k}^{[s]}$ ,  $c \neq 0$ . We consider symmetric symbol energies and fourth moments:

$$\begin{aligned} E &= \langle |X_m^{[s]}|^2 \rangle = \langle |\bar{X}_m^{[s]}|^2 \rangle, \quad \text{all } s, m \\ E_c &= \langle |B_{c,k}^{[s]}|^2 \rangle = \langle |\bar{B}_{c,k}^{[s]}|^2 \rangle, \quad \text{all } s, k, c \neq 0 \\ Q_c &= \langle |B_{c,k}^{[s]}|^4 \rangle = \langle |\bar{B}_{c,k}^{[s]}|^4 \rangle, \quad \text{all } s, k, c \neq 0. \end{aligned} \quad (9)$$

The receiver applies a band-pass filter  $h_{\mathcal{B}}(t)$  followed by linear distortion compensation (LDC) or digital back-propagation (DBP), a matched filter, and a sampler:

$$y_m^{[s]} = \int_{-\infty}^{\infty} s_0^*(t - mT) \left\{ \mathcal{D}_{-\mathcal{L}}^{[s]} \left[ h_{\mathcal{B}}(t) * u^{[s]}(\mathcal{L}, t) \right] \right\} dt. \quad (10)$$

We focus on  $y_m^{[s]}$  to save space. Due to symmetry, the model for  $\bar{y}_m^{[s]}$  is obtained by replacing all variables with a ‘‘bar’’ by the corresponding variables without a ‘‘bar’’, and vice versa. We assume that  $h_{\mathcal{B}}(t) * s(t) = s(t)$ .

Substituting (4) into (10), and using (8), we obtain the RP model of the received symbols:

$$y_m^{[s]} = x_m^{[s]} + w_m^{[s]} + \Delta x_m^{[s]}. \quad (11)$$

As in [20], the noise  $w_m^{[s]}$  is independent and identically distributed (i.i.d.) complex Gaussian with variance  $N_{\text{ASE}}$ . Also as in [20], we neglect signal-noise mixing, and the nonlinear interference (NLI) becomes

$$\begin{aligned} \Delta x_m^{[s]} &= j \sum_{s'} \sum_{\substack{n \\ k, k'}} S_{n,k,k'}^{[s,s']} x_{n+m}^{[s]} x_{k+m}^{[s']} x_{k'+m}^{[s']*} \\ &\quad + j \sum_{s'} \sum_{\substack{n \\ k, k'}} \tilde{S}_{n,k,k'}^{[s,s']} \bar{x}_{n+m}^{[s]} \bar{x}_{k+m}^{[s']} \bar{x}_{k'+m}^{[s']*} \\ &\quad + j \sum_{s'} \sum_{c \neq 0} \sum_{\substack{n \\ k, k'}} C_{c;n,k,k'}^{[s,s']} x_{n+m}^{[s]} b_{c,k+m}^{[s']} b_{c,k'+m}^{[s']*} \\ &\quad + j \sum_{s'} \sum_{c \neq 0} \sum_{\substack{n \\ k, k'}} \tilde{C}_{c;n,k,k'}^{[s,s']} \bar{x}_{n+m}^{[s]} \bar{b}_{c,k+m}^{[s']} \bar{b}_{c,k'+m}^{[s']*} \\ &\quad + j \sum_{r \neq s} \sum_{c \neq 0} \sum_{\substack{n \\ k, k'}} D_{c;n,k,k'}^{[s,r]} x_{n+m}^{[r]} b_{c,k+m}^{[s]} b_{c,k'+m}^{[s']*} \\ &\quad + j \sum_{s'} \sum_{c \neq 0} \sum_{\substack{n \\ k, k'}} \tilde{D}_{c;n,k,k'}^{[s,s']} \bar{x}_{n+m}^{[s']} \bar{b}_{c,k+m}^{[s]} \bar{b}_{c,k'+m}^{[s']*}. \end{aligned} \quad (12)$$

The coefficients in (12) can be written in terms of

$$\begin{aligned} A_{n,k,k'}^{[s,s']}(t_1, t_2, t_3) &= \gamma f_{s,s'} \int_0^{\mathcal{L}} dz g_{s'}(z) \int_{-\infty}^{\infty} dt s^*(z, t) \\ &\quad s(z, t - nT - t_1) s(z, t - kT - t_2) s^*(t - k'T - t_3). \end{aligned} \quad (13)$$

We choose  $\tau_0^{[s]} = 0$ . For  $r \neq s$ , we have

$$S_{n,k,k'}^{[s,s']} = A_{n,k,k'}^{[s,s']}(0, \tau_0^{[s]}, \tau_0^{[s']}) \quad (14)$$

$$\tilde{S}_{n,k,k'}^{[s,s']} = A_{n,k,k'}^{[s,s']}(0, \bar{\tau}_0^{[s]}, \bar{\tau}_0^{[s']}) \quad (15)$$

$$C_{c;n,k,k'}^{[s,s]} = 2A_{n,k,k'}^{[s,s]}(0, \tau_c^{[s]} - \beta_2^{[s]} \Omega_c z, \tau_c^{[s]} - \beta_2^{[s]} \Omega_c z) \quad (16)$$

$$C_{c;n,k,k'}^{[s,r]} = A_{n,k,k'}^{[s,r]}(0, \tau_c^{[r]} - \beta_2^{[r]} \Omega_c z, \tau_c^{[r]} - \beta_2^{[r]} \Omega_c z) \quad (17)$$

$$\tilde{C}_{c;n,k,k'}^{[s,s']} = A_{n,k,k'}^{[s,s']}(0, \bar{\tau}_c^{[s]} - \beta_2^{[s]} \Omega_c z, \bar{\tau}_c^{[s]} - \beta_2^{[s]} \Omega_c z) \quad (18)$$

$$D_{c;n,k,k'}^{[s,r]} = A_{n,k,k'}^{[s,r]}(\tau_0^{[r]}, \tau_c^{[s]} - \beta_2^{[s]} \Omega_c z, \tau_c^{[r]} - \beta_2^{[r]} \Omega_c z) \quad (19)$$

$$\tilde{D}_{c;n,k,k'}^{[s,s']} = A_{n,k,k'}^{[s,s']}(\bar{\tau}_0^{[s]}, \tau_c^{[s]} - \beta_2^{[s]} \Omega_c z, \bar{\tau}_c^{[s]} - \beta_2^{[s]} \Omega_c z). \quad (20)$$

Using single-polarization DBP on the COI removes the terms with  $S_{n,k,k'}^{[s,s']}$  from (12). Using dual-polarization DBP on the COI removes the terms with  $S_{n,k,k'}^{[s,s]}$  or  $\tilde{S}_{n,k,k'}^{[s,s]}$ . Using multi-mode DBP removes all terms with  $S_{n,k,k'}^{[s,s']}$  or  $\tilde{S}_{n,k,k'}^{[s,s]}$ .

#### IV. SDM-CRAN MODEL

As in [20], we gather all terms from (12) that depend on the current symbols. Assuming multi-mode DBP, we write

$$\begin{pmatrix} \Delta x_m^{[1]} \\ \overline{\Delta x}_m^{[1]} \\ \vdots \\ \Delta x_m^{[S]} \\ \overline{\Delta x}_m^{[S]} \end{pmatrix} = j\mathbf{J}_m \begin{pmatrix} x_m^{[1]} \\ \overline{x}_m^{[1]} \\ \vdots \\ x_m^{[S]} \\ \overline{x}_m^{[S]} \end{pmatrix} + \begin{pmatrix} v_m^{[1]} \\ \overline{v}_m^{[1]} \\ \vdots \\ v_m^{[S]} \\ \overline{v}_m^{[S]} \end{pmatrix} \quad (21)$$

where  $\mathbf{J}_m$  is defined block-wise as

$$\mathbf{J}_m = \begin{pmatrix} \mathbf{D}_m^{[1,1]} & \mathbf{B}_m^{[1,2]} & \dots & \mathbf{B}_m^{[1,S]} \\ \mathbf{B}_m^{[2,1]} & \mathbf{D}_m^{[2,2]} & \ddots & \mathbf{B}_m^{[2,S]} \\ \vdots & \ddots & \ddots & \vdots \\ \mathbf{B}_m^{[S,1]} & \mathbf{B}_m^{[S,2]} & \dots & \mathbf{D}_m^{[S,S]} \end{pmatrix}. \quad (22)$$

The diagonal blocks (of size  $2 \times 2$ ) are

$$\mathbf{D}_m^{[s,s]} = \begin{pmatrix} \theta_m^{[s]} & \psi_m^{[s,s]} \\ \overline{\psi}_m^{[s,s]} & \overline{\theta}_m^{[s]} \end{pmatrix} \quad (23)$$

and the off-diagonal blocks are

$$\mathbf{B}_m^{[s,r]} = \begin{pmatrix} \xi_m^{[s,r]} & \psi_m^{[s,r]} \\ \overline{\psi}_m^{[s,r]} & \overline{\xi}_m^{[s,r]} \end{pmatrix} \quad (24)$$

where, for  $r \neq s$ , we have

$$\begin{aligned} \theta_m^{[s]} &= \sum_{s'} \sum_{c \neq 0} \sum_{k, k'} C_{c;0,k,k'}^{[s,s']} b_{c,k+m}^{[s']} b_{c,k'+m}^{[s']*} \\ &+ \sum_{s'} \sum_{c \neq 0} \sum_{k, k'} \tilde{C}_{c;0,k,k'}^{[s,s']} \overline{b}_{c,k+m}^{[s']} \overline{b}_{c,k'+m}^{[s']*} \end{aligned} \quad (25)$$

$$\psi_m^{[s,s']} = \sum_{c \neq 0} \sum_{k, k'} \tilde{D}_{c;0,k,k'}^{[s,s']} b_{c,k+m}^{[s]} \overline{b}_{c,k'+m}^{[s']*}. \quad (26)$$

$$\xi_m^{[s,r]} = \sum_{c \neq 0} \sum_{k, k'} D_{c;0,k,k'}^{[s,r]} b_{c,k+m}^{[s]} b_{c,k'+m}^{[r]*}. \quad (27)$$

and  $\overline{\theta}_m^{[s]}$ ,  $\overline{\psi}_m^{[s,s']}$ , and  $\overline{\xi}_m^{[s,r]}$  are obtained by swapping  $b_{c,\ell}^{[i]}$  with  $\overline{b}_{c,\ell}^{[i]}$  in (25)-(27), swapping  $\tau_c^{[i]}$  with  $\overline{\tau}_c^{[i]}$  in (14)-(20), and shifting all delays such that  $\overline{\tau}_0^{[s]} = 0$ . The residual NLI terms  $v_m^{[s]}$  and  $\overline{v}_m^{[s]}$  are given by (12) without the two first lines (in the DBP case) and without the summands with  $n = 0$ .

We choose all pulses of the same frequency channel to be synchronized, i.e., we set  $\tau_c^{[s]} = \overline{\tau}_c^{[s]} := \tau_c$  for all  $s$  and  $c$ .<sup>2</sup> We thus have  $\tilde{D}_{c;0,k,k'}^{[s,s']} = \tilde{D}_{c;0,k',k}^{[s',s]*}$ ,  $D_{c;0,k,k'}^{[s,s']} = D_{c;0,k',k}^{[s',s]*}$ , and

$$\psi_m^{[s,s']} = \overline{\psi}_m^{[s',s]*}, \quad \xi_m^{[s,r]} = \xi_m^{[r,s]*}, \quad \overline{\xi}_m^{[s,r]} = \overline{\xi}_m^{[r,s]*}. \quad (28)$$

Since the  $\theta_m^{[s]}$  and  $\overline{\theta}_m^{[s]}$  are real [20], the matrix  $\mathbf{J}_m$  is Hermitian. Using (25)-(27), it follows that all the diagonal terms  $\Theta_m^{[s]}$  and  $\overline{\Theta}_m^{[s]}$  are correlated and all other crosscorrelations are 0.

<sup>2</sup>For multi-carrier transmission, the  $2S$  pulses of each subcarrier are synchronized but the pulses of different subcarriers are not.

#### A. Mode Rotation Approximation

As in [20], we apply an LP-like approximation

$$\mathbf{I} + j\mathbf{J}_m \approx \exp(j\mathbf{J}_m). \quad (29)$$

Using (21) and (11), we write the SDM-CRAN model as

$$\mathbf{y}_m = \exp(j\mathbf{J}_m) \mathbf{x}_m + \mathbf{v}_m + \mathbf{w}_m \quad (30)$$

where  $\mathbf{y}_m = (y_m^{[1]}, \overline{y}_m^{[1]}, \dots, y_m^{[S]}, \overline{y}_m^{[S]})^T$ , and  $\mathbf{x}_m$ ,  $\mathbf{v}_m$ , and  $\mathbf{w}_m$  are defined similarly. The matrix  $\exp(j\mathbf{J}_m) \in \mathbb{C}^{2S \times 2S}$  is unitary. The components of the residual NLI  $\mathbf{v}_m$  are uncorrelated and have memory in the time parameter  $m$ , see [20]. The statistics of the entries of  $\mathbf{J}_m$  can be derived as in [20]. We state results for strong coupling next.

#### B. Statistics of $\mathbf{J}_m$ for Strong Coupling

Strong coupling has  $f_{s,s'} = \kappa$ ,  $\beta_2^{[s]} = \beta_2$  and  $g_s(z) = g(z)$ . Furthermore, all the coefficients of the same frequency channel  $c$ , except for  $C_{c;n,k,k'}^{[s,s]}$ , are equal and independent of  $s, s'$ , and  $r$ . We call these coefficients  $X_{c;n,k,k'}$ :

$$\begin{aligned} X_{c;n,k,k'} &:= \frac{C_{c;n,k,k'}^{[s,s]}}{2} = C_{c;n,k,k'}^{[s,r]} = \tilde{C}_{c;n,k,k'}^{[s,s']} \\ &= D_{c;n,k,k'}^{[s,r]} = \tilde{D}_{c;n,k,k'}^{[s,s']} \end{aligned} \quad (31)$$

for all  $s, s'$  and all  $r \neq s$ . The means of the entries  $J_{i,k}[m]$  of the matrix  $\mathbf{J}_m$  in (30) are

$$\langle J_{i,i}[m] \rangle = (1 + 2S) \sum_{c \neq 0} E_c \sum_k X_{c;0,k,k'} \quad (32)$$

$$\langle J_{i,k}[m] \rangle = 0, \quad k \neq i. \quad (33)$$

The auto- and crosscovariance functions of the  $J_{i,k}[m]$  can be written in terms of the following two functions:

$$\begin{aligned} r[\ell] &= \sum_{c \neq 0} (Q_c - E_c^2) \sum_k X_{c;0,k,k} X_{c;0,k-\ell,k-\ell} \\ &+ \sum_{c \neq 0} E_c^2 \sum_{k \neq k'} X_{c;0,k,k'} X_{c;0,k-\ell,k'-\ell} \end{aligned} \quad (34)$$

$$s[\ell] = \sum_{c \neq 0} E_c^2 \sum_{k,k'} X_{c;0,k,k'} X_{c;0,k-\ell,k'-\ell}. \quad (35)$$

If one defines

$$r_{ik'i'k'}[\ell] = \langle J_{i,k}[m] J_{i',k'}^*[m+\ell] \rangle - \langle J_{i,k}[m] \rangle \langle J_{i',k'}^*[m+\ell] \rangle \quad (36)$$

then the autocovariance functions are

$$r_{iiii}[\ell] = (3 + 2S)r[\ell] \quad (37)$$

$$r_{ikik}[\ell] = s[\ell], \quad k \neq i; \quad (38)$$

the crosscovariance function of two diagonal elements is

$$r_{iikk}[\ell] = (2 + 2S)r[\ell], \quad k \neq i; \quad (39)$$

and the other crosscorrelation functions are 0:

$$r_{iii'k'}[\ell] = 0, \quad i' \neq k' \quad (40)$$

$$r_{ik'i'k'}[\ell] = 0, \quad (i, k) \neq (i', k') \text{ and } (i, k) \neq (k', i') \quad (41)$$

where we recall that  $\mathbf{J}_m$  is Hermitian. If the inputs  $B_{c,k}^{[s]}$  and  $\overline{B}_{c,k}^{[s]}$  are CSCG, then we have  $r[\ell] = s[\ell]$ . In the limit of large

accumulated dispersion, the approximations introduced in [23] apply (see [19], [20]):

$$\langle J_{i,i}[m] \rangle \approx (1 + 2S)\gamma\kappa \frac{\mathcal{L}}{T} \sum_{c \neq 0} E_c \quad (42)$$

$$r[\ell] \approx \frac{\gamma^2 \kappa^2 \mathcal{L}}{T} \sum_{c \neq 0} \frac{Q_c - E_c^2}{|\beta_2 \Omega_c|} \left[ 1 - \frac{|\ell|T}{|\beta_2 \Omega_c| \mathcal{L}} \right]^+ \quad (43)$$

$$s[\ell] \approx \frac{\gamma^2 \kappa^2 \mathcal{L}}{T} \sum_{c \neq 0} \frac{E_c^2}{|\beta_2 \Omega_c|} \left[ 1 - \frac{|\ell|T}{|\beta_2 \Omega_c| \mathcal{L}} \right]^+ \quad (44)$$

where one assumes that the contributions of the summands with  $X_{c;0,k,k}$  in (34) and (35) dominate, see [20, Fig. 2]. For example, in a 2-pol system ( $S = 1$ ), the ACF  $r_\Theta[\ell]$  of the diagonal elements of  $\mathbf{J}_m$  is  $5r[\ell]$  (see (37)), with  $r[\ell]$  approximately given by (43). This matches [20, Eq. (75)].

## V. SIMPLIFIED SDM-CRAN MODEL

In the following, the receiver removes the means  $\langle \Theta_m^{[s]} \rangle \equiv \langle J_{2s-1,2s-1}[m] \rangle$  and  $\langle \bar{\Theta}_m^{[s]} \rangle \equiv \langle J_{2s,2s}[m] \rangle$  of the phase noise, and we abuse notation and write  $J_{i,i}[m]$  for the resulting zero-mean variables. Based on the statistical analysis of Section IV-B, we model the entries of the matrix  $\mathbf{J}_m$  in (30) as

$$j_{i,i}[m] = 2\phi_i[m] + \sum_{i' \neq i} \phi_{i'}[m] \quad (45)$$

$$j_{k,i}[m] = j_{i,k}^*[m] \quad (46)$$

where the  $\Phi_i[m]$ ,  $i = 1, \dots, 2S$ , are independent, real, Gaussian, memory- $\mu$  Markov processes generated using the procedure in [20, Section IV.B] with autocovariance function  $r[\ell]$  in (34) for  $\ell \in \{-\mu, \dots, \mu\}$ . The  $J_{i,k}[m]$  for  $i < k$  are independent CSCG memory- $\mu$  Markov processes generated using the same procedure with autocovariance function  $s[\ell]$  in (35) for  $\ell \in \{-\mu, \dots, \mu\}$ . The number of hidden independent *real* Markov processes in  $\mathbf{J}_m$  is thus  $4S^2$ , of which  $2S$  are the  $\Phi_i[m]$ .

As in [19], [20], we combine the ASE noise and the residual NLI noise into one additive noise term  $\mathbf{z}_m = \mathbf{v}_m + \mathbf{w}_m$ . The simplified (mismatched) SDM-CRAN model is

$$\mathbf{y}_m = \exp(j\mathbf{J}_m) \mathbf{x}_m + \mathbf{z}_m. \quad (47)$$

We model the entries  $Z_i[m]$  of  $\mathbf{z}_m$  as independent CSCG processes with real ACFs

$$r_{Z_i}[\ell] := \langle Z_i[m] Z_i^*[m + \ell] \rangle = N_{\text{ASE}} \delta[\ell] + \langle V_i[m] V_i^*[m + \ell] \rangle \quad (48)$$

where  $v_i[m]$  is the  $i$ -th entry of  $\mathbf{v}_m$ . The ACF  $r_{Z_i}[\ell]$  has short memory and a similar shape as [19, Fig. 3].

## VI. NUMERICAL RESULTS

### A. Estimating Model Parameters

We use a training set to estimate the parameters of the model (47). Since the matrix  $\exp(j\mathbf{J}_m)$  in (47) is unitary, if we use i.i.d. Gaussian inputs  $\mathbf{x}_m$  and neglect the small correlations in  $\mathbf{Z}_m$  then the distribution of  $\|\mathbf{Y}_m\|^2$  given  $\|\mathbf{X}_m\|$  is noncentral chi-squared with  $4S$  degrees of freedom,

TABLE I  
SYSTEM PARAMETERS

Parameter	Symbol	Value
Dispersion coefficient	$\beta_2$	$-21.7 \text{ ps}^2/\text{km}$
Nonlinear coefficient	$\gamma$	$1.27 \text{ W}^{-1} \text{ km}^{-1}$
RX noise spectral density	$N_{\text{ASE}}$	$5.902 \cdot 10^{-18} \text{ W/Hz}$
Number of spatial modes	$S$	2
WDM channel indexes	$c_{\min}, c_{\max}$	-2, 2
Transmitted pulse shape	$s(t)$	sinc
Channel bandwidth	$\mathcal{B}$	50 GHz
Channel spacing	$\Omega^{(1)}/(2\pi)$	50 GHz

and independent for each  $m$ . We thus estimate the noise variance  $\sigma_Z^2 = r_{Z_i}[0]$  as

$$\hat{\sigma}_Z^2 = \arg \max_{\sigma^2} \sum_m \log \left[ \frac{e^{-\frac{\|\mathbf{y}_m\|^2 + \|\mathbf{x}_m\|^2}{\sigma^2}} \|\mathbf{y}_m\|^{2S-1}}{\sigma^2 \|\mathbf{x}_m\|^{2S-1}} I_{2S-1} \left( \frac{2\|\mathbf{y}_m\| \|\mathbf{x}_m\|}{\sigma^2} \right) \right]. \quad (49)$$

We estimate the mean phase noise  $\langle J_{i,i}[m] \rangle$  as in [20]. For the matrix  $\mathbf{J}_m$ , we assume that all  $\Phi_i[m]$  (see (45)) have the same ACF  $\sigma_\Phi^2 r[\ell]$ , and that all  $J_{k,i}[m]$  for  $k < i$  have the same ACF  $\sigma_J^2 s[\ell]$ , with  $r[\ell]$  and  $s[\ell]$  given by (43) and (44). We minimize the mismatched conditional entropy  $h_q(\mathbf{Y}|\mathbf{X})$  (obtained using particle filtering [20]) over  $\sigma_\Phi^2$  and  $\sigma_J^2$ . We use the same symmetric, real, three-tap, unit-energy whitening filter on all modes, and minimize  $h_q(\mathbf{Y}|\mathbf{X})$  over its free parameter.

### B. Achievable Rates

We simulated the strong coupling system (3) with  $S = 2$  spatial modes and 5 WDM channels by using the split-step Fourier method. The system has IDA and the parameters in Table I. As in [20], we compare single- and multi-carrier systems, where the latter system has four subcarriers (4SC) of bandwidth 12.5 GHz each. All subcarriers have the same power, i.e., there is no frequency-dependent power allocation as in [19], [20]. The input symbols have a Gaussian density. The channel delays  $\tau_c$  are chosen randomly between  $-T/2$  and  $T/2$ . The receiver applies a 50-GHz band-pass filter to isolate the COI, followed by joint DBP on all COI spatial modes and subcarriers, and then matched filtering and sampling. A training set of 24 sequences of 4092 symbols (20 sequences of  $4 \times 1023$  symbols in the 4SC system) is used to estimate the SDM-CRAN model parameters.

We apply particle filtering on a test set of 120 sequences (100 sequences for 4SC) to compute achievable rates as described in [20, Sec. VI]. The mismatched output distribution is Gaussian [20, Eq. (91)]. The results are plotted in Fig. 1 that compares four receiver algorithms with successively more complex processing:

- separate processing of each of the  $2S$  (complex-alphabet) channels using a memoryless mismatched model with i.i.d. phase-and-additive noise, see [19, Sec. VIII.A];
- separate 1-pol CPAN (1pCPAN) processing of each of the  $2S$  channels with  $2S$  particle filters, see [19];

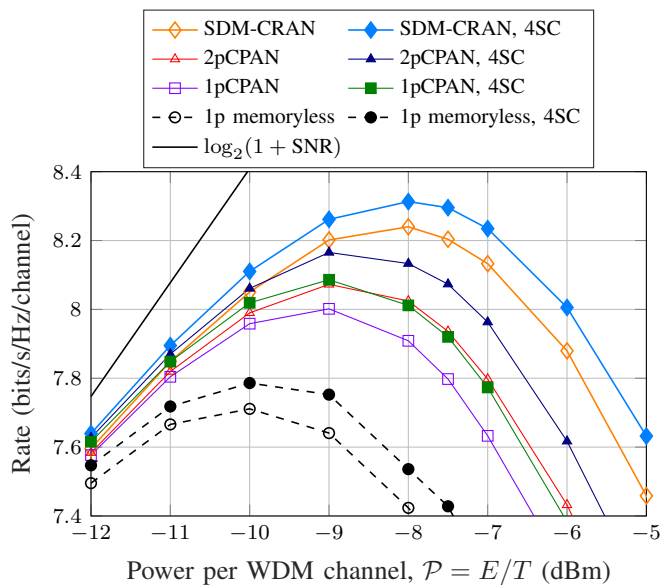


Fig. 1. Achievable rates for a 1000-km SDM link with  $S = 2$  spatial modes, 5 WDM channels, strong coupling, and the parameters in Table I. SNR =  $P/(N_{ASE}B)$

- separate 2-pol CPAN (2pCPAN) processing of the  $S$  spatial modes with  $S$  particle filters, see [20];
- joint CRAN processing of all  $2S$  channels with one particle filter that uses the mismatched model (45)–(48).

With respect to memoryless processing, the 1pCPAN model gains 0.29 bits/s/Hz/channel, the 2pCPAN model gains a further 0.07 bits/s/Hz/channel, and the SDM-CRAN model gains another 0.17 bits/s/Hz/channel. 4SC gains between 0.07 and 0.1 bits/s/Hz/channel with respect to single-carrier transmission. The rate gain from the peak of the lowermost curve to the peak of the uppermost curve is approximately 0.6 bits/s/Hz/channel. The rate gain from “Memoryless” to “SDM-CRAN” for either single- or multi-carrier transmission is 0.5 bits/s/Hz/channel. For 4SC, the power gain from the rate peak with memoryless processing to the SDM-CRAN curve at the same rate (7.79 bits/s/Hz/channel) is 1.4 dB.

## VII. CONCLUSIONS

We extended the analysis of the CPAN model [19], [20] to SDM for weak and strong coupling. The SDM-CRAN model and a multi-carrier scheme were applied to strong coupling to obtain achievable rates for a  $S = 2$  spatial mode system. The rates are 0.6 bits/s/Hz/channel larger than the rates for a single-carrier system with separate and memoryless processing per complex-alphabet channel.

We remark that computational complexity limits the numerical calculations to a small number  $S$  of spatial modes. An important direction for future work is speeding up the calculations and designing simplified receivers that exploit the correlations predicted by the SDM-CRAN model in practical multi-mode systems. An interesting theory question is to extend the LP analyses of [14]–[16] to SDM.

## REFERENCES

- [1] D. J. Richardson, J. M. Fini, and L. E. Nelson, “Space-division multiplexing in optical fibres,” *Nature Photonics*, vol. 7, pp. 354–362, Apr. 2013.
- [2] D. Soma *et al.*, “10.16 peta-bit/s dense SDM/WDM transmission over low-DMD 6-mode 19-core fibre across C+L band,” in *Eur. Conf. Optical Commun. (ECOC)*, 2017.
- [3] R. Ryf *et al.*, “Transmission over randomly-coupled 4-core fiber in field-deployed multi-core fiber cable,” in *Eur. Conf. Optical Commun. (ECOC)*, 2020.
- [4] R. S. Luís *et al.*, “Experimental demonstration of a petabit per second SDM network node,” *J. Lightw. Technol.*, vol. 38, no. 11, pp. 2886–2896, Jun. 2020.
- [5] G. Kramer, M. I. Yousefi, and F. R. Kschischang, “Upper bound on the capacity of a cascade of nonlinear and noisy channels,” in *IEEE Inf. Theory Workshop*, Apr. 2015.
- [6] M. I. Yousefi, G. Kramer, and F. R. Kschischang, “Upper bound on the capacity of the nonlinear Schrödinger channel,” in *IEEE Can. Workshop Inf. Theory*, Jul. 2015, pp. 22–26.
- [7] R. J. Essiambre, G. Kramer, P. J. Winzer, G. J. Foschini, and B. Goebel, “Capacity limits of optical fiber networks,” *J. Lightw. Technol.*, vol. 28, no. 4, pp. 662–701, Feb. 2010.
- [8] P. Poggiolini, G. Bosco, A. Carena, V. Curri, Y. Jiang, and F. Forghieri, “The GN-model of fiber non-linear propagation and its applications,” *J. Lightw. Technol.*, vol. 32, no. 4, pp. 694–721, Feb. 2014.
- [9] A. Carena, G. Bosco, V. Curri, Y. Jiang, P. Poggiolini, and F. Forghieri, “EGN model of non-linear fiber propagation,” *Opt. Express*, vol. 22, no. 13, pp. 16 335–16 362, Jun. 2014.
- [10] A. Mecozzi, C. B. Clausen, and M. Shtaif, “Analysis of intrachannel nonlinear effects in highly dispersed optical pulse transmission,” *IEEE Photon. Technol. Lett.*, vol. 12, no. 4, pp. 392–394, Apr. 2000.
- [11] —, “System impact of intra-channel nonlinear effects in highly dispersed optical pulse transmission,” *IEEE Photon. Technol. Lett.*, vol. 12, no. 12, pp. 1633–1635, Dec. 2000.
- [12] A. Vannucci, P. Serena, and A. Bononi, “The RP method: a new tool for the iterative solution of the nonlinear Schrödinger equation,” *J. Lightw. Technol.*, vol. 20, no. 7, pp. 1102–1112, Jul. 2002.
- [13] A. Mecozzi and R. Essiambre, “Nonlinear Shannon limit in pseudolinear coherent systems,” *J. Lightw. Technol.*, vol. 30, no. 12, pp. 2011–2024, Jun. 2012.
- [14] E. Ciaramella and E. Forestieri, “Analytical approximation of nonlinear distortions,” *IEEE Phot. Technol. Lett.*, vol. 17, no. 1, pp. 91–93, Jan. 2005.
- [15] E. Forestieri and M. Secondini, “Solving the nonlinear Schrödinger equation,” in *Optical Communication Theory and Techniques*, E. Forestieri, Ed. Boston, MA: Springer, 2005, pp. 3–11.
- [16] M. Secondini, E. Forestieri, and C. R. Menyuk, “A combined regular-logarithmic perturbation method for signal-noise interaction in amplified optical systems,” *J. Lightw. Technol.*, vol. 27, no. 16, pp. 3358–3369, Aug. 2009.
- [17] M. Secondini, E. Forestieri, and G. Prati, “Achievable information rate in nonlinear WDM fiber-optic systems with arbitrary modulation formats and dispersion maps,” *J. Lightw. Technol.*, vol. 31, no. 23, pp. 3839–3852, Dec. 2013.
- [18] M. Secondini, E. Agrell, E. Forestieri, D. Marsella, and M. R. Camara, “Nonlinearity mitigation in WDM systems: Models, strategies, and achievable rates,” *J. Lightw. Technol.*, vol. 37, no. 10, pp. 2270–2283, May 2019.
- [19] F. J. García-Gómez and G. Kramer, “Mismatched models to lower bound the capacity of optical fiber channels,” *J. Lightw. Technol.*, vol. 38, no. 24, pp. 6779–6787, Dec. 2020.
- [20] F. J. García-Gómez and G. Kramer, “Mismatched models to lower bound the capacity of dual-polarization optical fiber channels,” *J. Lightw. Technol.*, vol. 39, no. 11, pp. 3390–3399, Jun. 2021.
- [21] S. Mumtaz, R.-J. Essiambre, and G. P. Agrawal, “Nonlinear propagation in multimode and multicore fibers: Generalization of the manakov equations,” *J. Lightw. Technol.*, vol. 31, no. 3, pp. 398–406, 2013.
- [22] A. Mecozzi, C. Antonelli, and M. Shtaif, “Coupled Manakov equations in multimode fibers with strongly coupled groups of modes,” *Opt. Express*, vol. 20, no. 21, pp. 23 436–23 441, Oct. 2012.
- [23] R. Dar, M. Feder, A. Mecozzi, and M. Shtaif, “Properties of nonlinear noise in long, dispersion-uncompensated fiber links,” *Opt. Express*, vol. 21, no. 22, pp. 25 685–25 699, Nov. 2013.